Solid Earth Discuss., 6, 1227–1264, 2014
www.solid-earth-discuss.net/6/1227/2014/
doi:10.5194/sed-6-1227-2014

Solid Earth
Discussions
Open Access

The rheological behavior of fracture-filling cherts: example of Barite Valley dikes, Barberton Greenstone Belt, South Africa

M. Ledevin, N. Arndt, and A. Simionovici

University Grenoble Alpes, ISTerre, 38041 Grenoble, France

Received: 7 April 2014 – Accepted: 15 April 2014 – Published: 13 May 2014

Correspondence to: M. Ledevin (morgane.ledevin@gmail.com)

Published by Copernicus Publications on behalf of the European Geosciences Union.

Abstract

A 100 m-thick complex of near-vertical carbonaceous chert dikes marks the transition from the Mendon to Mapepe Formations (3260 Ma) in the Barberton Greenstone Belt, South Africa. Fracturing was intense in this area, as shown by the profusion and width of the dikes (ca. 1 m on average) and by the abundance of completely shattered rocks. The dike-and-sill organization of the fracture network and the upward narrowing of some of the large veins indicate that at least part of the fluid originated at depth and migrated upward in this hydrothermal plumbing system.

Abundant angular fragments of silicified country rock are suspended and uniformly distributed within the larger dikes. Jigsaw-fit structures and confined bursting textures indicate that hydraulic fracturing was at the origin of the veins. The confinement of the dike system beneath an impact spherule bed suggests that the hydrothermal circulations were triggered by the impact and located at the external margin of a large crater.

From the geometry of the dikes and the petrography of the cherts, we infer that the fluid that invaded the fractures was thixotropic. On one hand, the injection of black chert into extremely fine fractures is evidence for low viscosity at the time of injection; on the other hand, the lack of closure of larger veins and the suspension of large fragments in a chert matrix provide evidence of high viscosity soon thereafter. The inference is that the viscosity of the injected fluid increased from low to high as the fluid velocity decreased. Such rheological behavior is characteristic of media composed of solid and colloidal particles suspended in a liquid. The presence of abundant clay-sized, rounded particles of silica, carbonaceous matter and clay minerals, the high proportion of siliceous matrix and the capacity of colloidal silica to form cohesive 3-D networks through gelation, account for the viscosity increase and thixotropic behavior of the fluid that filled the veins. Stirring and shearing of the siliceous mush as it was injected imparted a low viscosity by decreasing internal particle interactions; then, as the flow rate declined, the fluid became highly viscous as the inter-particulate bonds (siloxane bonds, Si-O-Si) were reconstituted. The gelation of the chert was rapid and

SED
6, 1227–1264, 2014

The rheological behavior of fracture-filling cherts

M. Ledevin et al.

the structure persisted at low temperature ($T < 200\,^{\circ}$C) before fractures were sealed and chert indurated.

1 Introduction

Siliceous sediments – cherts and banded iron formations – are common in many Archean greenstone belts. Normally they occur as conformable units, intercalated with or replacing volcanic units or clastic metasediments; in some regions, however, they occur as crosscutting dikes (e.g. Lowe and Knauth, 1977; Nijman et al., 1998; Lowe and Byerly, 2003; Lowe et al., 2003; Hofmann, 2005; de Vries et al., 2006; de Wit et al., 2011). Such successions are recognized in greenstone belts worldwide, the best-preserved and least metamorphosed being in the Pilbara in Western Australia and the Barberton belt in South Africa (e.g. Lowe and Knauth, 1977; Nijman et al., 1998; Lowe and Byerly, 2003; Lowe et al., 2003; de Vries et al., 2006; de Wit et al., 2011). The origin of these dikes remains controversial (e.g. Lowe and Knauth, 1977; Nijman et al., 1998; Lowe and Byerly, 2003; Lowe et al., 2003; Orberger et al., 2006; Hofmann and Bolhar, 2007; Hofmann and Harris, 2008).

Hofmann and Bolhar (2007) and Lowe (2013) conducted extensive fieldwork and petrographic studies in the Barite Valley syncline of the Barberton Greenstone belt that led to contrasting theories for the origin of the dikes. The first authors interpreted chert-invaded volcano-sedimentary successions in the area as a fossilized hydrothermal system. They propose a model in which the dikes represent the roots of shallow low-temperature hydrothermal cells within the Archean oceanic crust. Hydraulic fracturing below an impermeable cap of chert accounts for the formation of fissures, then the downward migration of still-soft seafloor sediments filled the now open fractures with a mixture of carbonaceous sediment and chemical precipitates. Lowe (2013) favored a model in which the impact of a large meteorite fractured the Archean seafloor and triggered dike formation. The author's model reaches that of Hofmann and Bolhar

(2007) in that the cherts were derived essentially from oceanic sediments that found their way down into the open fractures.

In this study we explore the nature of the chert that filled the dikes and focus on its rheology at the time it was injected. Through our descriptions of the field relations and dike geometry, and of the macro- and microscopic characteristics of the chert, we demonstrate that the fluids from which the chert formed had unusual thixotropic behavior.

2 Geological context and location of studied dikes

The Barberton Greenstone Belt is a 3.57–3.21 Ga volcano-sedimentary sequence typical of Archean greenstone belts, beginning with the highly metamorphosed Sandspruit and Theespruit Formations, followed by the thick, volcanic-dominated Onverwacht Group (3530–3334 Ma; Viljoen and Viljoen, 1969b, a; Armstrong et al., 1990; Kröner et al., 1991; Lowe and Byerly, 1999). This sequence terminates with largely mafic-ultramafic volcanics of the Kromberg and Mendon Formations (e.g. Viljoen and Viljoen, 1969c; Armstrong et al., 1990; Kröner et al., 1991; Kamo and Davis, 1994; Byerly et al., 1996; Lowe and Byerly, 1999). The overlying Fig Tree Group marks an evolution to more felsic rocks with increasing sediment contributions of clastic or chemical deposits (3258–3226 Ma; e.g. Kröner et al., 1991; Byerly et al., 1993; Lowe and Nocita, 1999; Hofmann, 2005). The sequence ends with the thick, clastic-dominated Moodies Group (3230–3110 Ma; e.g. Kröner et al., 1991; Kamo and Davis, 1994; Furnes et al., 2011; Heubeck et al., 2013), essentially composed of the erosional products of previously deposited Fig Tree and Onverwacht Groups.

The Barite Valley site is located north-east of the Onverwacht anticline (Fig. 1a) where the uppermost units of the Mendon Formation (Onverwacht Group; 3335–3260 Ma; Kröner et al., 1991; Byerly et al., 1993, 1996) are conformably overlain by the lowermost units of the Mapepe Formation (Fig Tree Group; 3260–3225 Ma; Armstrong et al., 1990; Byerly et al., 1996). The Onverwacht to Fig Tree transition is well exposed

SED
6, 1227–1264, 2014

on the western limb of the Barite Valley syncline (Lowe, 2013). Here, the Mendon Formation comprises a series of komatiite flows (Figs. 1b and 2) with highly silicified upper parts (Duchac and Hanor, 1987; Hanor and Duchac, 1990; Hofmann and Harris, 2008; Lowe, 2013), which evolve to a 100 m-thick unit of thinly laminated ferruginous cherts (Mc1), massive to thickly bedded black cherts (Mc2) and greenish micaceous cherts (Mc3), all deposited in a quiet, probably deep, subaqueous environment (Lowe, 2013).

Felsic pyroclastic and volcaniclastic sediments of the Mapepe Fm. conformably overlie these units (Figs. 1b and 2). The base of this sequence is marked by a layer containing spherules, named S2 by Lowe and Byerly (1986b), which represents a regional marker across the Barberton belt. Spherules are quenched liquid silicate droplets interpreted as meteorite impact products based on their form and lithology, their platinum-group-element content (Lowe and Byerly, 1986b; Lowe et al., 1989, 2003), and their non-terrestrial chromium isotopic ratios (Shokolyukov et al., 2000; Kyte et al., 2003). Dating of a tuff deposit a few meters above S2 gives an age of about 3260 Ma for the impact that produced the spherules (Kröner et al., 1991).

The following Mapepe units comprise intervals of lithic sandstone, chert-slab conglomerate, barite and minor chert, jasper layers and mudstone (Heinrichs, 1980; Lowe, 1999, 2013; Lowe and Nocita, 1999). They resulted from clastic sedimentation in shallow environments, evolving from fan-delta to alluvial and shallow marine to non-marine conditions (Lowe and Nocita, 1999; Lowe, 2013). Part of the detritus, especially the chert clasts in conglomerates, was derived from the underlying Mendon Formation (Lowe, 2013).

The sedimentary units are folded and dip steeply to the S–SE (Fig. 3a). At the top of the Mendon Formation, cream-to-white bedded tuffaceous cherts are cut by the veins of black chert that are the focus of this study (Figs. 2 and 3) (Lowe and Nocita, 1999; Lowe and Braunstein, 2003; Lowe et al., 2003; Lowe, 2013). The veins terminate below the spherule bed S2 of the overlying Mapepe unit (Lowe and Byerly, 1986b; Lowe, 2013). Some fractures are parallel to the bedding of the enclosing tuffs and commonly root in larger and discordant dikes that can be followed for 100 m into the underlying

SED
6, 1227–1264, 2014

Mendon komatiitic units. Most of the dykes were near vertical when they formed. Typical examples are illustrated in Fig. 3b and c.

3 Chert dikes

3.1 Geometry of fractures

As shown in Figs. 1b, 2 and 3a, the dike complex is first encountered in the komatiitic volcanic rocks of the Mendon Fm., as described by Lowe (2013). They can be followed upward through the overlying laminated, ferruginous cherts of M1c unit, then through the black cherts from Mc2, to terminate in the greenish micaceous cherts of unit Mc3, below the spherule bed S2. In average, the fractures become narrower with depth in the Mendon Formation. The dikes are oriented to the W–NW and cut across the sedimentary rocks at high angle, normally at 60 to 90° to the bedding although Lowe (2013) has reported values as low as 20–40°.

The fractures display a wide range of shapes, widths and fracture intensities as illustrated in Fig. 4. They vary in thickness from a few centimeters to several meters (0.5 to 1 m in average) and have complex structures in which numerous mm-thick veins branch out from the main part of fractures. In the sequence illustrated in photos (a) to (d) of Fig. 4, the shape evolves from straight dikes to irregular fractures, the intermediate shapes (b) and (c) being the most common type encountered in the area.

The fractures are in sharp contact with surrounding banded cream to white cherts and contain variable amounts of host rock fragments embedded within a black chert matrix. The fragments are most commonly angular in shape, although sub-rounded to rounded examples are observed (see next section and Figs. 7 and 8 for descriptions). The resulting structure is either matrix-supported (Fig. 4b) or clast-supported (Fig. 4c) depending on the clast-to-matrix ratio and degree of fracturing.

Intense fracturing is illustrated by the clast-supported texture of Fig. 5. The structure consists of little displaced, minimally rotated, sub-angular to angular clasts of fine-grained cream to white country rock separated by < 1 mm to cm wide veins of black chert. All clasts are elongated in about the same direction due to the sub-parallel orientation of most of the chert veins, and the fragments form a "jigsaw-puzzle" texture. The fracturing was more intense in the upper part of the structures (Fig. 5a) as shown by the greater abundance of small fragments (typically < 5 mm). In the lower part of the structures (Fig. 5b), the chert veins are larger and country rock fragments are bigger. These fragments appear to be suspended in the siliceous matrix, at least in the two-dimensional view of the outcrop.

Other examples of highly fractured zones are shown in Fig. 6. In photo (a), the texture resembles the jigsaw-puzzle of the veins shown in Fig. 5, but the fragments are slightly more rounded. Black chert veins are abundant and range in size from < 1 mm to 5 mm. Photo (b) differs from (a) by showing multiple thin veins that spread out at 360° from a highly fractured central zone.

3.2 Internal structures

Although some of the dikes are filled entirely with homogeneous, translucent black chert (Fig. 4a), at a finer scale it is seen that most are charged with fragments originating from the enclosing banded cream to white cherts. As shown in Fig. 7, the fragments have polyhedral, spindle-like shapes covering a wide range of forms between angular to sub-rounded. They vary in size from < 1 cm to 40–50 cm (< 10 cm in average) (see also Fig. 4b–d) and are uniformly distributed within the dike with their long dimensions commonly sub-parallel to the fracture walls (Fig. 7b and d), especially when close to the contact.

The finest and roundest particles we found are shown in Fig. 8. They form dense packages at the bottom of a sill (b) or between suspended fragments in the main vertical channel (c). The rounded particles are less than 1 mm in diameter and composed of pure, translucent silica. Such particles are rare and most of small fragments (< 1 cm) display sub-rounded to sharp edges similar to larger clasts (e.g. Fig. 4d).

SED
6, 1227–1264, 2014

Title Page
Abstract Introduction
Conclusions References
Tables Figures
◀| |▶
◀ ▶
Back Close
Full Screen / Esc
Printer-friendly Version
Interactive Discussion

The origin of fragments is readily establishing due to their resemblance with surrounding bedded tuffs in terms of color, grain size, structure and texture. We estimate that more than 90 % of the clasts are derived from the adjacent units. The laminations of the source rock are generally preserved in clasts (e.g. Fig. 4c), except for the most silicified examples. In Fig. 7c, the darker zones show signs of interaction with siliceous fluids as highlighted by the partial disappearance of primary structures.

The distribution of country rock fragments varies from one dike to another. The jigsaw structures shown in Fig. 5 have the highest clast to matrix ratio and all the fragments are close to one another, being separated only by thin veins of black chert. These clasts are much longer than they are wide, and comprise more than 60–70 % of the fractured zone; the black chert matrix is restricted to thin veins with a typical width of less than 1 mm.

In larger dikes, the proportion of clasts is more variable. The transition from clast- to matrix-supported is not obvious, being limited by the two-dimension of outcrops, but a typical example of a matrix-supported dike is shown in Fig. 7, photo (d) (see also Fig. 4b for a larger view). In this dike, pale grey blocks of country rock are suspended in the black chert matrix together with multiple clasts of translucent black chert (Fig. 7d).

In other examples of matrix-supported dikes, the black chert matrix appears homogeneous and free of macroscopic fragments, as in Fig. 4a. Other examples are shown in Fig. 9, where host rock fragments are rare or absent. In this dike, silica precipitated to form either botryoidal columnar structures perpendicular to the fracture wall (Fig. 9a), or colloform structures manifested by alternating thin black-and-white laminations (< 0.5 mm thick; Fig. 9c). In Fig. 9b, colloform textures form the core of the fracture whereas the contact with country rocks is marked by a 2 to 3 cm thick zone of white, translucent silica.

SED
6, 1227–1264, 2014

4 Microscopic observations

The petrography of two representative fracture-filling cherts is shown in Fig. 10a and b. These samples were collected in matrix-supported fractures that cut through pale grey tuffaceous cherts from the Mc2 unit, which are essentially composed of sericite and microquartz with a variable amount of Fe-carbonate.

The apparent homogeneity of the chert in outcrop does not apply at a microscopic scale. The sample illustrated in Fig. 10a is in fact a microbreccia made up of small fragments of chert, now composed of microcrystalline quartz (> 90 %), and a few percent of carbonaceous material, in a microquartzitic matrix. The proportion of matrix is difficult to determine but is estimated between 20 and 30 %. The grains of carbonaceous matter are rounded and consist of fine aggregates usually less than 100 µm in size, with rare, larger aggregates up to 300 µm. The microscopic fragments of chert are angular to well rounded – almost spherical – and they range in size from 200–300 µm. They are in close contact to one another and are composed of microquartz very similar to that in the surrounding matrix.

The sample in Fig. 10b comprises a mixture of small rounded grains of silica, carbonaceous matter and carbonate set in a very fine microquartzitic matrix. This sample differs from the previous one by having a more abundant matrix (up to 60 %) whose dark color is due to the presence of diffuse carbonaceous matter. The grains of carbonaceous material comprise half of the particulate fraction. They have sub-rounded shapes and range in size from 10 to 500 µm (100 µm in average). Silica grains form the rest of the particulate fraction and display sub-rounded shapes similar to the carbonaceous grains. They are composed of almost pure microquartz (< 5–10 µm) in either sharp or diffusive contact with the surrounding matrix. Fe-rich dolomite (MgO = 15–17 wt%; FeO = 7–9 wt%) is a minor component (< 5 %) and is found as isolated, rhombohedral to rounded grains no larger than 50 µm.

The boundaries of chert dikes are commonly lined by a thin layer of relatively pure silica, the best examples of which are shown in Fig. 11. These contacts are charac-

SED
6, 1227–1264, 2014

terized, first by a very thin silica layer less than 50 µm thick in contact with country rocks, then by a variably thick layer (up to 1 mm) of coarser silica showing two types of textures: (1) well-preserved colloform textures now composed of microquartz with thin lines of phyllosilicates and/or carbonaceous matter (Fig. 11a), and (2) crystal growth structures perpendicular to the fracture walls and surrounded by relatively pure microquartz (Fig. 11b). The contact with the fracture-filling chert is either sharp (Fig. 11a) or diffuse (Fig. 11b), and commonly followed by an interval rich in rounded, pure silica grains.

5 Discussion

Two main theories have been proposed to explain the formation of chert dikes and the intense fracturing observed in the Barite Valley Syncline, both based on extensive field mapping, analysis of dike geometry and structure, and petrographic observations.

The "hydraulic fracturing hypothesis" was proposed by Hofmann and Bolhar (2007) who argue that the sedimentary units of Upper Mendon Fm were silicified during or just after deposition by pervasive and diffuse circulation of low-temperature hydrothermal fluids through the seafloor. The resulting impermeable cap of chert acted like the seal of a pressure cooker, increasing the pressure of trapped fluids in the hydrothermal system and leading to extensive fracturing and dike formation.

Lowe and Byerly (2003) and Lowe (2013) proposed that the impact of one or more meteorites or asteroids at ca. 3260–3240 Ma supplied sufficient energy to intensely fracture the ocean crust. Their model includes contemporaneous crustal fracturing and tectonic activity leading to local block displacement, dike formation and tsunami generation, all related to the impact spherule bed S2 (Lowe and Byerly, 1986b)

The following section focuses mainly on the rheology of the fluids that precipitated the chert that fills the fractures. A discussion of the mechanism of dike formation is beyond the scope of this study, but both the above hypotheses will be briefly discussed because the fracturing and the origin of the circulating fluid may be closely related.

5.1 Filling of the fracture: from below or from above?

Although the hydraulic and impact hypotheses invoke different fracturing mechanisms, they concur on the following point: the fractures are filled from above, by the downward migration of unconsolidated carbonaceous sediments of the Mc2 and Mc3 divisions. According to Hofmann and Bolhar (2007) and Lowe (2013), these sediments were present on the seafloor at the time of dike formation and migrated as soft and/or liquefied material into the newly formed, open fractures. The main arguments advocated are (1) the presence of rock fragments in dikes from higher stratigraphic levels, and an absense of fragments from lower stratigraphic levels, (2) the downward displacement of blocks eroded from adjacent country rocks and (3) the geometry of the dike complex which is 50 m wide at the top and extends as individual dikes downward into the Mendon volcanic units.

Although we concur with most of these observations and interpretations, Fig. 12 shows evidence of (pene-)contemporaneous upward fluid migration in some of the dikes that we studied. Photo (a) shows a dike-and-sill structure similar to those observed in magmatic plumbing systems. The main, vertical channel spreads out laterally at specific sedimentary intervals (i.e. weaker planes) to form horizontal veins (or sills) concordant with host rock bedding. The structure does not persist upward but ends with a final sill of limited lateral extent (< 40 cm). Another example comes from the multi-branch dike of photo (b) where the main channel, or feeder channel, is largest at the base and narrower when cutting through younger units. The central part of the dike contains suspended host rock fragments that are displaced (∼ 1 cm) toward the top of the fracture.

Both these structures provide evidence that some fluids came from below. However, we show in the following section that minor upward fluid is compatible with the dominantly downward flow inferred by Lowe (2013).

5.2 Rheological behavior of the circulating fluids

Arguably the most important finding of this study centers on the physical characteristics of the fluid that filled the fractures. In Sect. 3.1, we showed several examples where the black chert occupies a network of fractures (e.g. jigsaw textures of Fig. 5) and penetrated into even the finest (< 1 mm) veins, indicating that the chert had low viscosity at the time it was injected. In contrast, very soon after injection, the same material appears to have acquired a viscosity high enough to suspend large blocks of country rock. In other words, the cherts exhibit thixotropic behavior (e.g. Bauer and Collins, 1967; Barnes, 1997; Mewis and Wagner, 2009). When the fluid was injected, the stirring and shearing imparted a low viscosity then, as the rate of movement decreased, the fluid became highly viscous.

The fact that blocks of country rock are distributed uniformly through the black chert in the large "matrix-supported" dikes (e.g. Fig. 4b) indicates that the transition from low to high viscosity was sufficiently rapid that the blocks did not have the time to settle towards the lower part of the fracture. This is especially noticeable in the jigsaw zones of Fig. 5, where the veins are wider in the bottom part of the structure and much thinner at the top. The lack of vein closure through the lower zone indicates that the blocks of country rock did not settle downwards and suggests again a rapid low to high viscosity transition.

5.3 The cause of thixotropic behavior

Inspection of thin sections shows that the matrix of fracture-filling black chert is not homogeneous but consists of an assemblage of fine rounded particles in a siliceous medium (Fig. 10). The significance of this finding is brought out by reference to the extensive literature on thixotropic systems.

Barnes (1997) and Mewis and Wagner (2009) (and reference therein) reported that thixotropy is typical of colloidal suspensions or any other system in which solid particles are suspended in a fluid. Examples of such materials are abundant in everyday life, including food products (e.g. yoghurt, mayonnaise, ketchup), pharmaceutical and personal care products, adhesives, paints, printing inks and so on (see references in Barnes, 1997; Mewis and Wagner, 2009). The clay slurries and silicate suspensions commonly used in mining industries are also strongly thixotropic (e.g. Nguyen and Boger, 1985; Besq et al., 2000; de Kretser and Boger, 2001; Klein and Hallbom, 2002; Oleksy et al., 2007).

Boswell (1948) showed that all unconsolidated sediments exhibit thixotropy to a greater or lesser extent. The degree of thixotropy depends on a variety of factors including (1) the size and shape of suspended particles, (2) the packing density and water content of the system, and (3) the presence of electrolytes such as seawater salts. Grain geometry is particularly important: Freundlich (1935), a pioneer of thixotropy, observed that a substantial proportion of platy fine-grained particles would cause the viscosity to drop under shear stress. He recognized that rounded shapes or significant amount of silt and/or sand in the particulate fraction does not inhibit the development of thixotropic behavior, although it lowers its efficiency.

In the siliceous matrix that the thixotropy of the fluid that filled the Barite Valley fractures can be linked directly to the presence of the small silica and carbonaceous particles randomly distributed in the siliceous matrix. Although the mechanism that produces viscosity variations in natural systems is debated, it is broadly accepted that the rheological behavior of particulate (or colloidal) suspensions is controlled by the competition between (1) the break-down of microstructures in the fluid under flow stresses and (2) the build-up of new microstructures favored by in-flow collisions and Brownian motion (Boswell, 1948; Barnes, 1997; Mewis and Wagner, 2009). In other words, when the slurry is stirred and the critical shear stress is exceeded, the attraction between particles is lowered and the viscosity drops to a minimum; as movement decreases, the attraction becomes stronger and the slurry more viscous.

Although the mechanism that colloidal suspensions, such as those produced at hydrothermal vents (e.g. Guidry and Chafetz, 2002, 2003; Channing et al., 2004; Tobler et al., 2008), attraction forces and viscosity increase are linked to the polymerization of small (nm) to large (µm) silica flocs to form coherent 3-D networks or gel-like structures (Iler, 1979; Williams and Crerar, 1985; Bergna, 1994; Channing et al., 2004). This process, called gelation, depends on the formation of branch chains in which hydroxyl groups (Si-OH) at the surface of colloidal silica combine to produce siloxane bonds (Si-O-Si). The polymerization is enhanced when silica flocs are associated with other solid particles that act as nuclei (Rimstidt and Barnes, 1980; Williams et al., 1985; Williams and Crerar, 1985; Rouchon and Orberger, 2008). Thus, the thixotropic behavior of the primary filling material is well explained by the characteristics of the fracture-filling cherts; i.e. the abundance of suspended silica flocs and rounded grains of carbonaceous matter and clay-sized particles eroded from the surrounding silicified tuffaceous country rocks. As the fluid stopped flowing in the veins, Si-O-Si bonds formed between suspended particles and colloidal silica, and the viscosity increased as the matrix was transformed into gel.

The timing of network formation and viscosity increase, and the strength of the newly formed network depend on several factors that influence the silica polymerization, including (1) the temperature, degree of supersaturation and acidity of the fluid (Iler, 1979; Chen and Marshall, 1982; Rimstidt and Cole, 1983; Fournier, 1985; Renaut et al., 2002; Renaut and Jones, 2003), (2) the extent of aggregation or disaggregation of particles in the fluid (Stade and Wicker, 1971; Dietzel, 2000; Chanson et al., 2006), and (3) the presence of activated complexes such as salts that help to balance the negatively charged silica colloids, especially in near-neutral and alkaline media (Marshall and Warakomski, 1980; Marshall and Chen, 1982; Dandurand et al., 1982; Yates et al., 1998; Grenne and Slack, 2003; Channing et al., 2004).

Recently, Hunt et al. (2013) conducted rheological experiments to quantify the gelation capacity of colloidal suspensions of silica in order to use such material in the generation of geothermal energy. Their results show that in colloidal solution containing 15–20 wt% SiO_2 gels can form within minutes to hours at temperatures of 175–200 °C, or within several days at lower temperatures (100–130 °C). Although the gelation time is faster above 200 °C, the gels are more stable at lower temperatures, where they survive

SED
6, 1227–1264, 2014

up to several months or years. Applied to the Barite Valley dikes, their study provides an idea of how would have behaved the silica in fractures. The abundance of silica in the fracture-filling chert suggests that the colloidal suspension that intruded the sediments initially had a silica content comparable to the fluids used by Hunt et al. (2013). The lack of sulphides and hematite coatings of fractures, together with the abundance of colloform and botryoidal silica, indicates that the fluid temperatures were less than 200 °C. Thus, based on the study of Hunt et al. (2013), we infer that the dike-filling fluid reached a gel-state very rapidly, probably within a day after its injection, and (2) that this gel remained stable for several months to years under medium-low temperature conditions. Such a rapid process can account for the lack of settling of country rock fragments as described in the previous section.

5.4 The timing and mechanism of dike formation

In this section we focus on the linkage between the process that produced the fractures and the process that introduced the chert-forming fluid. From our observations, it is possible to reconcile the hydraulic and impact hypotheses of Hofmann and Bolhar (2007) and Lowe (2013).

For reasons outlined above and developed below, we believe that hydraulic fracturing was the main process that shattered the rock. The key argument centers on our conclusion that the time between the development of the fractures and their infilling with chert was very short. The lack of settling of matrix-supported blocks (Fig. 4b) and the lack of closure of the fracture networks even in the lower part of the fractures (Fig. 5b) points to rapid influx of a low viscosity fluid that was able to invade the entire fracture network. We suggest that unless the fractures were kept open by overpressured fluid, or perhaps by the presence of particles in the fluid (in the manner of sand injected during hydraulic fracturing for shale gas extraction), the fractures would close. The latter process would only operate for fractures whose widths were no more that a few times the diameter of the particles; i.e. less than a millimeter.

Such rapid influx of fluid seems inconsistent with the model of Lowe (2013) who suggested that the fractures remained open for a considerable time based on their observation of cavity-filling textures – botryoidal silica at cavity margins grading inwards to coarser quartz crystals – and sediment accumulation features at the borders of fractures. He argued that the lower parts of the largest fractures remained open longer than their upper parts, and that soft sediments descended slowly to the deepest levels of the fractures. In our opinion, the formation of impact-triggered open fractures on the seafloor fails to explain (1) the lack of clast settling and their suspension in the black chert matrix, (2) the constancy of fracture thickness in lower parts of highly fractured zones (Fig. 5b) and (3) the in-situ disintegration of country rocks inferred from both the jigsaw structures (Fig. 5) and the 360° dispersion of some vein networks (Fig. 6).

For these reasons we propose that the fluid that precipitated the chert was the same as that which shattered the rock. We support the model of Hofmann and Bolhar (2007) who suggested that a layer of silicified rocks formed an impermeable cap that allowed pressure to build up in the fluids confined to the underlying substrate. Once the pressure exceeded the strength limit of the confining rocks, they shattered, opening passageways into which was injected a slurry of fine, abraded particles of country rock in a colloidal solution. Overpressure in the fluid kept open the fractures until the flow velocity decreased and the viscosity increased to a level sufficient to suspend the fractured blocks of country rocks. In cases where the fractures reached the surface, relaxation of the system soon after its emplacement and before its complete induration allowed the migration of surface sediments into the newly formed fractures.

The nature of the fracturing mechanism remains unclear. Nijman (1998) proposed seafloor hydrothermalism for a setting similar to the present study – the ca. 3.5 Ga North Pole Chert from the Pilbara greenstone belt, Western Australia. He concluded that similar dikes were produced by the upward flow of hydrothermal fluids rich in silica, barium and carbonaceous matter. Lowe (2013) recognized that similar Ba-rich fluids could account for the barite layers in the Mapepe Fm in Barite Valley (e.g. Heinrich, 1980; Lowe and Nocita, 1999), a conclusion consistent with Hofmann and Bolhar's

(2007) image of an extensive, low temperature and shallow hydrothermal system confined beneath a shallow layer of lithified and silicified cherts. However, Lowe (2013) argued that the development of the fractures were linked directly to meteorite impacts.

We suggest that impact-induced hydrothermalism at the far edge of a crater could account for most of the observations made in the area. Lowe (2013) infers that the crater at the origin of the impact spherule bed S2 could be many hundreds of meters in width, and that the Barite Valley dike system extended possibly 4 to 5 times farther than the crater diameter, an assessment based essentially on the lack of coarse detritus in the S2 spherule layer. It has been shown from studies of other craters that impact-derived hydrothermal systems can form within and outside the collapsed transient cavity (e.g. Naumov, 2002; Abramov and Kring, 2005). Concentric and radial fault systems, as well as normal faults, develop in the marginal collapse zone because of (1) the seismic shaking resulting from the initial impact, and (2) the destabilization of crater boundaries due to the newly created free border. These weak zones are ideal pathways for fluids heated below the impact zone, thus leading to the formation of deep to shallow fractures and vent systems at the surface. Faults and hydrothermal systems are observed at distances up to several times the crater diameter (e.g. Spray and Thompson, 1995; Spray, 1998; Spray et al., 2004; Osinski et al., 2005; Rodriguez et al., 2005). Thus, it seems reasonable to attribute the dike formation at Barite Valley to post-impact fluid flow along a normal fault system that developed beyond a main crater.

Such a model meets the criteria imposed by the observations made in the area and reconciles the theories of Hofmann and Bolhar (2007) and Lowe (2013).

(1) The geometry of the dikes, being sub-vertical- to vertical and narrowing either downward or upward across the sedimentary units, is consistent with fracturing processes that operated in the shallow crust. Evidence for upward fluid migration in dikes (e.g. the dike-and-sill geometry), followed by episodes when sediments settled into the fractures, favors the following two-step model: during or soon after the impact, hot overpressured fluids were extracted through hydraulic fracturing in the external zones

SED
6, 1227–1264, 2014

of the crater, then the collapse of the crater and relaxation of the system allowed soft sediments to sink into some of the newly opened fractures.

(2) The fracturing process may have been facilitated by the formation of a thixotropic silica gel layer along the fracture walls. Lubrification of faults by colloidal silica (Goldsby and Tullis, 2002; Di Toro et al., 2004; Beeler, 2009; Hayashi and Tsutsumi, 2010) may also have occurred in the Barite Valley dikes. The presence of colloform silica layers at the boundary with country rocks, in places associated with crystal growth structures (Fig. 11), can be interpreted as remnants of frictionally generated amorphous silica now crystallized to microquartz.

(3) The precipitation of colloform and botryoidal silica in the internal parts of some dikes records the presence of low temperature Si-rich fluids within the stability field of chalcedony (typically below $<$ 150–200 °C). The formation of barite deposits and the widespread silicification of surface sediments at stratigraphic levels post-dating dike formation support the presence of significant hydrothermal venting at the seafloor. Silica enrichment in primary fluids, together with the lack of sulphide deposits (Ni, Cu) and hematite coatings of fractures, provides further evidence that the system was located far from the main impact zone.

(4) The restriction of chert dikes beneath the spherule layer (Hofmann and Bolhar, 2007; Lowe et al., 2003; Lowe, 2013), the rotation of large blocks separated by normal faults and mini-basins, the common occurrence of large dikes along these faults, and the generation of tsunamis soon after the fracturing (Lowe, 2013) can all be related to the impact and are all consistent with events observed in the marginal collapse zones of craters worldwide (e.g. Spray and Thompson, 1995; Spray, 1998; Naumov, 2002; Spray et al., 2004; Abramov and Kring, 2005; Rodriguez et al., 2005).

SED
6, 1227–1264, 2014

6 Conclusions

Based on the geometry of Barite Valley dikes and on the petrology of the fracture-filling cherts, several conclusions were reached concerning the mechanism of fracture formation and the nature and behavior of the pervasive fluid.

1. Impact-induced hydrothermalism and hydraulic fracturing by overpressured fluids account for the intense in situ brecciation of the country rocks. The plumbing system probably developed at low temperature at the external edge of a large crater.

2. The fluid that caused the fracturing was thixotropic, having a very low viscosity as it was injected and becoming highly viscous after circulation stopped. The presence of abundant clay-sized particles within the Si-rich fluid, and the capacity of silica-rich colloidal fluid to form cohesive 3-D networks, accounts for the viscosity variations.

3. Relaxation in part of the siliceous plumbing system allowed the collapse and downward migration of unconsolidated soft siliceous ooze from the seafloor into the fractures.

Acknowledgements. We thank the EPOV program (CNRS) and the ANR project BEGDy (BLAN-0109) for their financial support. We acknowledge Frédérique Pignon, Anne Davaille and François Renard for sharing their expertise in rheological concepts and for improving the manuscript. For the help in the lab at ISTerre, we thank Etienne Jaillard who contributed to thin section interpretations, and for the help in the field, we thank Axel Hofmann and Gordon Chunnett.

References

Abramov, O. and Kring, D. A.: Impact-induced hydrothermal activity on early Mars, J. Geophys. Res., 110, 2156–2202, 2005.

Armstrong, R. A., Compston, W., de Wit, M. J., and Williams, I. S.: The Stratigraphy of the 3.5–3.2 Ga Barberton greenstone belt revisited: a single zircon microprobe study, Earth Planet. Sc. Lett., 101, 90–106, 1990.

SED

6, 1227–1264, 2014

The rheological behavior of fracture-filling cherts

M. Ledevin et al.

Awramik, S. M., Schopf, J. W., and Walter, M. R.: Filamentous fossil bacteria 3.5 Gy old from the Archean of Western Australia, Precambrian Res., 20, 357–374, 1983.
Barnes, H. A.: Thixotropy – a review, J. Non-Newton. Fluid, 70, 1–33, 1997.
Bauer, W. H. and Collins, E. A.: Chapter 8, in: Rheology: Theory and Applications, edited by: Eirich, F. R., Academic Press, New York, 8, 423–459, 1967.
Bergna, H. E.: Colloidal chemistry of silica: an overview, In: The Colloidal Chemistry of Silica, edited by: Bergna, H. E., American Chemical Society, Advances in Chemistry Series, 234, 1–47, 1994.
Besq, A., Monnet, P., and Pantet, A.: Flow Situations of Drilling Muds – Effects of Thixotropic Property, Flucome Euro, 2000.
Boswell, P. G. H.: A preliminary examination of the thixotropy of sedimentary rocks, Quarterly Journal of the Geological Society, 104, 499–526, 1948.
Brandl, G., Cloete, M., and Anaeusser, C. R.: Archaean greenstone belts, in: The Geology of South africa, edited by: Johnson, M. R., Anhaeusser, C. R., and Thomas, R. J., Geological Society of South Africa, Johannesburg/Council for Geosciences, Pretoria, 9–15, 2006.
Byerly, G. R., Kröner, A., Lowe, D. R., and Walsh, M. M.: Sequential magmatic evolution of the early Archean Onverwacht Group: evidence from the upper formations, Eos T. Am. Geophys. Un., 74, 660 pp., 1993.
Byerly, G. R., Kröner, A., Lowe, D. R., Todt, W., and Walsh, M. M.: Prolonged magmatism and time constraints for sediment deposition in the early Archean Barberton greenstone belt: evidence from the Upper Onverwacht and Fig Tree groups, Precambrian Res., 78, 125–138, 1996.
Channing, A., Edwards, D., and Sturtevant, S.: A geothermally influenced wetland containing unconsolidated geochemical sediments, Can. J. Earth Sci., 41, 809–827, 2004.
Chanson, H., Jarny, S., and Coussot, P.: Dam break wave of thixotropic fluid, J. Hydraul. Eng.-ASCE, 132, 280–293, 2006.
Chen, C.-T. A. and Marshall, W. L.: Amorphous silica solubilities IV. Behavior in pure water and aqueous sodium chloride, sodium sulfate, magnesium chloride, and magnesium sulfate solutions up to 350 °C, Geochim. Cosmochim. Ac., 46, 279–287, 1982.
Dandurand, J. L., Schott, J. L., and Tardy, Y.: Solubilité de la silice dans des solutions aqueuses très concentrées de formamide et chlorure de lithium, Détermination du coefficient d'activité de la silice en solution, Bulletin of Mineralogy, 105, 357–363, 1982.

SED
6, 1227–1264, 2014

de Kretser, R. G. and Boger, D. V.: A structural model for the time-dependent recovery of mineral suspensions, Rheol. Acta, 40, 582–590, 2001.
de Vries, S. T., Nijman, W., and Armstrong, R. A.: Growth-fault structure and stratigraphic architecture of the Buck Ridge volcano-sedimentary complex, upper Hooggenoeg Formation, Barberton Greenstone Belt, South Africa, Precambrian Res., 149, 77–98, 2006.
de Wit, M. J., Hart, R. J., Martin, A., and Abbott, P.: Archaean abiogenic and probable biogenic structures associated with mineralized hydrothermal vent systems and regional metasomatism, with implications for greenstone belt studies, Econ. Geol., 77, 1783–1802, 1982.
de Wit, M. J., Furnes, H., and Robins, B.: Geology and Tectonostratigraphy of the Onverwacht Suite, Barberton Greenstone Belt, South Africa, Precambrian Res., 168, 1–27, 2011.
Di Toro, G., Goldsby, D. L., and Tullis, T. E.: Friction falls towards zero in quartz rock as slip velocity approaches seismic rates, Nature, 427, 436–439, 2004.
Dietzel, M.: Dissolution of silicates and the stability of polysilicic acid, Geochim. Cosmochim. Ac., 64, 3275–3281, 2000.
Duchac, K. C. and Hanor, J. S.: Origin and timing of the metasomatic silicification of an early archean komatiite sequence, barberton mountain land, South Africa, Precambrian Res., 37, 125–146, 1987.
Fournier, R. O.: The behavior of silica in hydrothermal solutions, in: Geology and Geochemistry of Epithermal Systems, edited by: Berger, B. R. and Bethke, P. M., Reviews in Economic Geology, vol. 2, 45–61, 1985.
Freundlich, H.: Thixotropy. The Colloidal State, Hermann, Paris, 267 pp., 1935.
Furnes, H., De Wit, M. J., Robins, B., and Sandståd, N. R.: Volcanic evolution of the upper Onverwacht Suite, Barberton Greenstone Belt, South Africa, Precambrian Res., 186, 28–50, 2011.
Goldsby, D. L. and Tullis, T. E.: Low frictional strength of quartz rocks at sub-seismic slip rates, Geophys. Res. Lett., 29, 25-1–25-4, 2002.
Grenne, T. and Slack, J. F.: Paleozoic and mesozoic silica-rich seawater: evidence from hematitic chert (jasper) deposits, Geology, 31, 319–322, 2003.
Guidry, S. A. and Chafetz, H. S.: Factors governing subaqueous siliceous sinter precipitation in hot springs: examples from Yellowstone National Park, USA, Sedimentology, 49, 1253–1267, 2002.
Guidry, S. A. and Chafetz, H. S.: Anatomy of siliceous hot springs: examples from Yellowstone National Park, Wyoming, USA, Sediment. Geol., 157, 71–106, 2003.

SED
6, 1227–1264, 2014

The rheological behavior of fracture-filling cherts

M. Ledevin et al.

Hanor, J. S. and Duchac, K. C.: Isovolumetric silicification of early Archean Komatities: geochemical mass balances and constraints on origin, J. Geol., 98, 863–877, 1990.
Hayashi, N. and Tsutsumi, A.: Deformation textures and mechanical behavior of a hydrated amorphous silica formed along an experimentally produced fault in chert, Geophys. Res. Lett., 37, L12305, doi:10.1029/2010GL042943, 2010.
Heinrichs, T.: Lithostratigraphische Untersuchungen in der Fig Tree Gruppe des Barberton Greenstone Belt zwischen Umsoli und Lomati (Südafrika), Göttinger Arbeiten zur Geologie und Paläontologie, 22, 118, 1980.
Heubeck, C. and Lowe, D. R.: Depositional and tectonic setting of the Archean Moodies Group, Barberton Greenstone Belt, South Africa, Precambrian Res., 68, 257–290, 1994.
Heubeck, C., Engelhardt, J., Byerly, G. R., Zeh, A., Sell, B., Luber, T., and Lowe, D. R.: Timing of deposition and deformation of the Moodies Group (Barberton Greenstone Belt, South Africa): very-high-resolution of Archaean surface processes, Precambrian Res., 231, 236–262, 2013.
Hofmann, A.: The geochemistry of sedimentary rocks from the Fig Tree Group, Barberton greenstone belt: implications for tectonic, hydrothermal and surface processes during mid-Archaean times, Precambrian Res., 143, 23–49, 2005.
Hofmann, A. and Bolhar, R.: Carbonaceous cherts in the Barberton Greenstone Belt and their significance for the study of early life in the Archean record, Astrobiology, 7, 355–388, 2007.
Hofmann, A. and Harris, C.: Silica alteration zones in the Barberton greenstone belt: a window into subseafloor processes 3.5–3.3 Ga ago, Chem. Geol., 257, 221–239, 2008.
Hofmann, A. and Wilson, A. H.: Silicified basalts, bedded cherts and other sea floor alteration phenomena of the 3.4 Ga Nondweni greenstone belt, South Africa, in: Earth's Oldest Rocks, edited by: Van Kranendonk. M. J., Smithies, R. H., and Bennett, V., Developments in Precambrian Geology, 15, 571–605, 2007.
Iler, R. K.: The Chemistry of Silica: Solubility, Polymerization, Colloid and Surface Properties, and Biochemistry, John Wiley and Sons Inc., New York, 1979.
Kamo, S. L. and Davis, D. W.: Reassessment of Archean crustal development in the Barberton Mountain Land, South Africa, based on U-Pb dating, Tectonics, 13, 167–192, 1994.
Klein, B. and Hallbom, D.: Modifying the rheology of nickel laterite suspensions, Miner. Eng., 15, 745–749, 2002.

SED
6, 1227–1264, 2014

Kröner, A., Byerly, G., and Lowe, D. R.: Chronology of Early Archean granite-greenstone evolution in the Barberton Mountain Land, South Africa, based on precise dating by signle zircon evaporation, Earth Planet. Sc. Lett., 103, 41–54, 1991.
Kyte, F. T., Shukolyukov, A., Lugmair, G. W., Lowe, D. R., and Byerly, G. R.: Early Archean spherule beds: chromium isotopes confirm origin through multiple impacts of projectiles of carbonaceous chondrite type, Geology, 31, 283–286, 2003.
Lowe, D. R.: Petrology and sedimentology of cherts and related silicified sedimentary rocks in the Swaziland Supergroup, in: Geological Evolution of the Barberton Greenstone Belt, South Africa, edited by: Lowe, D. R. and Byerly, G. R., Geol. S. Am. S., 329, 83–114, 1999.
Lowe, D. R.: Crustal fracturing and chert dike formation triggered by large meteorite impacts, ca. 3.260 Ga, Barberton greenstone belt, South Africa, Geol. Soc. Am. Bull., 125, 894–912, 2013.
Lowe, D. R. and Braunstein, D.: Microstructure of high-temperature (> 73 °C) siliceous sinter deposited around hot springs and geysers, Yellowstone National Park: the role of biological and abiological processes in sedimentation, Can. J. Earth Sci., 40, 1611–1642, 2003.
Lowe, D. R. and Byerly, G. R.: Archaean flow-top alteration zones formed initially in a low temperature sulphate-rich environment, Nature, 324, 245–248, 1986a.
Lowe, D. R. and Byerly, G. R.: Early Archean silicate spherules of probable impact origin, South Africa and Western Australia, Geology, 14, 83–86, 1986b.
Lowe, D. R. and Byerly, G. R.: Stratigraphy of the west-central part of the Barberton Greenstone Belt, South Africa, in: Geologic Evolution of the Barberton Greenstone Belt, South Africa, edited by: Lowe, D. R. and Byerly, G. R., Geol. S. Am. S., 329, 1–37, 1999.
Lowe, D. R. and Byerly, G. R.: Field Guide to the Geology of the 3.5–3.2 Ga Barberton Greenstone Belt, South Africa, Guidebook prepared for Field Conference: Archean Surface Processes, 184, 2003.
Lowe, D. R. and Knauth, L. P.: Sedimentology of the Onverwacht Group (3.4 billion years), Transvaal, South Africa, and its bearing on the characteristics and evolution of the early earth, J. Geol., 85, 699–723, 1977.
Lowe, D. R. and Nocita, B. W.: Foreland basin sedimentation in the Mapepe Formation, southern-facies Fig Tree Group, Geol. S. Am. S., 329, 233–258, 1999.
Lowe, D. R., Byerly, G. R., Asaro, F., and Kyte, F.: Geological and geochemical record of 3400-million year-old terrestrial meteorite impacts, Science, 245, 959–962, 1989.

SED
6, 1227–1264, 2014
The rheological behavior of fracture-filling cherts
M. Ledevin et al.

Lowe, D. R., Byerly, G. R., Kyte, F. T., Shukolyukov, A., Asaro, F., and Krull, A.: Spherule beds 3.47–3.24 billion years old in the Barberton Greenstone Belt, South Africa: a record of large meteorite impacts and their influence on early crustal and biological evolution, Astrobiology, 3, 7–48, 2003.
Marshall, W. L. and Chen, C.-T. A.: Amorphous silica soluhilities V. Predictions of solubility behavior in aqueous mixed electrolyte solutions to 300 °C, Geochim. Cosmochim. Ac., 46, 289–291, 1982.
Marshall, W. L. and Warakomski, J. M.: Amorphous silica solubilities – II. Effect of aqueous salt solutions at 25 °C, Geochim. Cosmochim. Ac., 44, 915–924, 1980.
Mewis, J. and Wagner, N. J.: Thixotropy, Adv. Colloid Interfac., 147–148, 214–227, 2009.
Naumov, M. V.: Impact-generated hydrothermal systems: data from Popagai, Kara, and Puchezh-Katunki impact structures, in: Impacts in Precambrian Shields, edited by: Plado, J. and Personen, L. J., 117–171, 2002.
Nguyen, Q. D. and Boger, D. V.: Thixotropic behaviour of concentrated bauxite residue suspensions, Rheol. Acta, 24, 427–437, 1985.
Nijman, W., de Bruijne, K. C., and Valkering, M. E.: Growth fault control of Early Archaean cherts, barite mounds and chert-barite veins, North Pole Dome, Eastern Pilbara, Western Australia, Precambrian Res., 88, 25–52, 1998.
Oleksy, M., Heneczkowski, M., and Galina, H.: Thixotropic compositions: unsaturated polyester resins/modified bentonites, Polimery, 52, 345–350, 2007.
Orberger, B., Rouchoun, V., Westall, F., de Vries, S. T., Pinti, D. L., Wagner, C., Wirth, R., and Hashizume, K.: Micro-facies and the origin of some Archean Cherts (Pilbara, Australia), Geol. S. Am. S., 405, 133–156, 2006.
Osinski, G. R., Lee, P., Spray, J. G., Parnell, J., Lim, D., Glass, B., Cockell, C. S., and Bunch, T. E. E.: Geological overview and cratering model for the Haughton impact structure, Devon Island, Canadian High Arctic, Meteorit. Planet. Sci., 40, 1759–1776, 2005.
Paris, I., Stanistreet, I. G., and Hughes, M. J.: Cherts of the Barberton Greenstone Belt interpreted as products of submarine exhalative activity, J. Geol., 93, 111–129, 1985.
Renaut, R. W. and Jones, B.: Sedimentology of hot spring systems, Can. J. Earth Sci., 40, 1439–1442, 2003.
Renaut, R. W., Jones, B., Tiercelin, J. J., and Tarits, C.: Sublacustrine precipitation of hydrothermal silica in rift lakes: evidence from Lake Baringo, centra Kenya Rift Valley, Sediment. Geol., 148, 235–257, 2002.

Rimstidt, J. D. and Barnes, H. L.: The kinetics of silica-water interaction, Geochim. Cosmochim. Ac., 44, 1683–1699, 1980.
Rimstidt, J. D. and Cole, D. R.: Geothermal mineralization 1: The mechanism of formation of the Beowawe, Nevada, siliceous sinter deposit, Am. J. Sci., 283, 861–875, 1983.
Rodriguez, J. A. P., Sasaki, S, Dohm, J. M., Tanaka, K. L., Strom, B., Kargel, J., Kuzmin, R., Miyamoto, H., Spray, J. G., Fairén, A. G., Komatsu, G., Kurita, K., and Baker, V.: Control of impact crater fracture systems on subsurface hydrology, ground subsidence, and collapse, Mars, J. Geophys. Res., 110, E06003, doi:10.1029/2004JE002365, 2005.
Rouchon, V. and Orberger, B.: Origin and mechanisms of K–Si-metasomatism of ca. 3.4–3.3 Ga volcaniclastic deposits and implications for Archean seawater evolution: examples from cherts of Kittys Gap (Pilbara craton, Australia) and Msauli (Barberton Greenstone Belt, South Africa), Precambrian Res., 165, 169–189, 2008.
Shukolyukov, A., Kyte, F. T., Lugmair, G. W., Lowe, D. R., and Byerly, G. R.: The oldest impact deposits on Earth – first confirmation of an extraterrestrial component, in: Impacts and the Early Earth, edited by: Gilmour, I. and Koeberl, C., Berlin, Springer-Verlag, 99–116, 2000.
Spray, J. G.: Pseudotachylyte type area: the Vredefort structure, South Africa, in: Fault-related Rocks: a Photographic Atlas, edited by: Snoke, A., Tullis, J., and Todd, V. R., Princeton University Press, Princeton, 76–79, 1998.
Spray, J. G. and Thompson, L. M.: Friction melt distribution in a multi-ring impact basin, Nature, 373, 130–132, 1995.
Spray, J. G., Butler, H. R., and Thompson, L. M.: Tectonic influences on the morphometry of the Sudbury impact structure: implications for terrestrial cratering and modeling, Meteorit. Planet. Sci., 39, 287–301, 2004.
Stade, H. and Wicker, W.: Zur Kinetik des Abbaus von Polykieselsäure $(H_2SiO_3)_x$ in wäßriger Lösung, Z. Anorg. Allg. Chem., 384, 53–56, 1971.
Tice, M. M. and Lowe, D. R.: The origin of carbonaceous matter in pre-3.0 Ga greenstone terrains: a review and new evidence from the 3.42 Ga Buck Reef Chert, Earth-Sci. Rev., 76, 259–300, 2006.
Tobler, D. J., Stefánsson, A., and Benning, L. G.: In-situ grown silica sinters in Icelandic geothermal areas, Geobiology, 6, 481–502, 2008.
Van Kranendonk, M. J.: Volcanic degassing, hydrothermal circulation and the flourishing of early life on Earth: a review of the evidence from ca. 3490–3240 Ma rocks of the Pilbara Supergroup, Pilbara Craton, Western Australia, Earth-Sci. Rev., 74, 197–240, 2006.

Viljoen, M. J. and Viljoen, R. P.: An introduction to the geology of the Barberton, granite-greenstone terrain, Geological Society of South Africa Special Publication, 9, 1–20, 1969a.
Viljoen, M. J. and Viljoen, R. P.: The geology and geochemistry of the lower ultramafic unit of the Onverwacht Group and a proposed new class of igneous rocks, Geological Society of South Africa Special Publication, 2, 55–86, 1969b.
Viljoen, M. J. and Viljoen, R. P.: The geological and geochemical significance of the upper formations of the Onverwacht Group, Upper Mantle Project, Special Publications of the Geological Society of South Africa, 2, 113–151, 1969c.
Walsh, M. M.: Microfossils and possible microfossils from the Early Archean Onverwacht Group, Barberton Mountain Land, South Africa. Precambrian Res., 54, 271–292, 1992.
Westall, F., de Wit, M. J., Dann, J., van der Gaast, S., de Ronde, C. E. J., and Gerneke, D.: Early Archean fossil bacteria and biofilms in hydrothermally-influenced sediments from the Barberton Greenstone belt, South Africa, Precambrian Res., 106, 93–116, 2001.
Williams, L. A. and Crerar, D. A.: Silica diagenesis; II, General mechanisms, J. Sediment. Res., 55, 312–321, 1985.
Williams, L. A., Parks, G. A., and Crerar, D. A.: Silica diagenesis, I. Solubility controls, J. Sediment. Petrol., 55, 301–311, 1985.
Yates, D. M., Joyce, K. J., and Heaney, P. J.: Complexation of copper with polymeric silica in aqueous solution, Appl. Geochem., 13, 235–241, 1998.

SED
6, 1227–1264, 2014

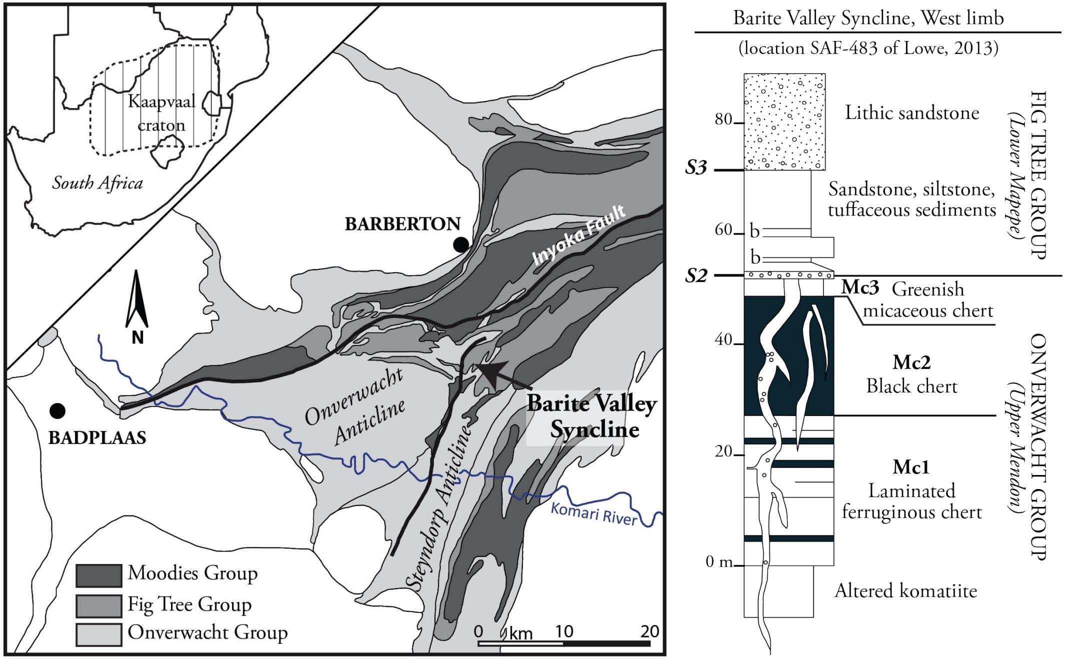

Fig. 1. (left) Simplified geological map of the Barberton Greenstone Belt and location of the Barite Valley Syncline north-east to the Onverwacht Anticline. (right) Stratigraphy modified from Lowe (2013) and corresponding to the western limb of the Barite Valley (location SAF-483 of Lowe, 2013). The Onverwacht to Fig Tree transition is marked by the spherule bed S2 (Lowe and Byerly, 1986b) below which is found the dike complex of this study. The dikes begin in the sedimentary units M3c and M2c, cut through M1c and extent down to the Si-metasomatised komatiitic flows.

SED
6, 1227–1264, 2014

The rheological behavior of fracture-filling cherts

M. Ledevin et al.

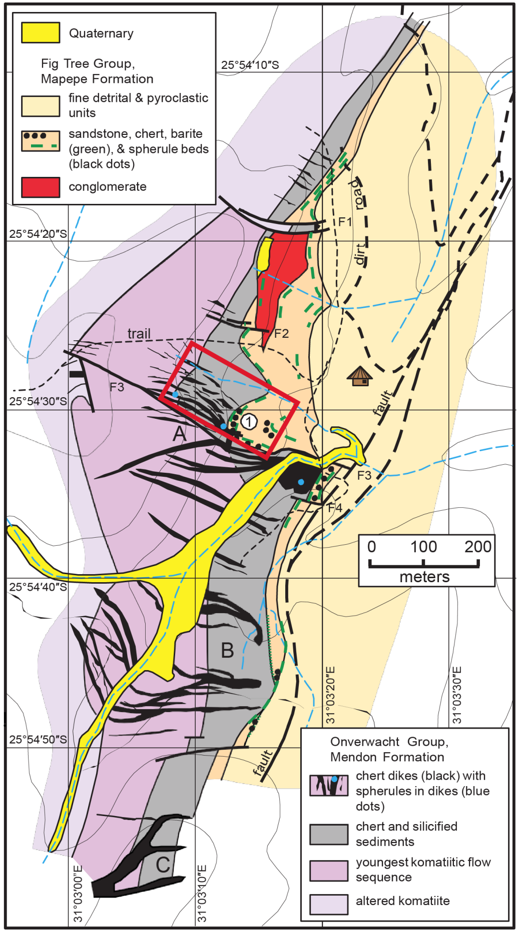

Fig. 2. Geological map of the Barite Valley site from Lowe (2013) showing the repartition of the dikes (black). They start at the top of the Mendon Formation (grey) and extent downward through to the komatiitic units (pink). The red rectangle represents the studied area.

SED
6, 1227–1264, 2014

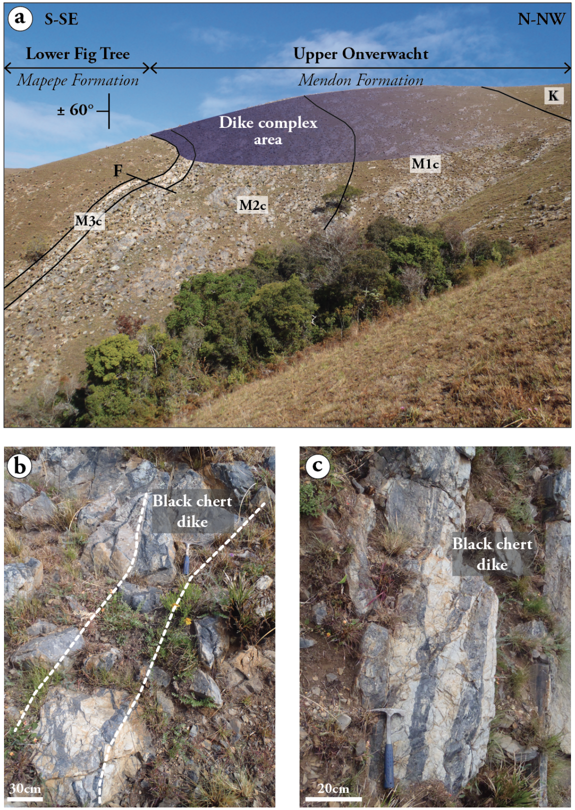

Fig. 3. (a) Photo of the Barite Valley area (NE side of the hill) showing the main limits of Mendon and Mapepe Formations. The series young to the S–SE and steeply deep at ±60° in the same direction. The main dike complex area begins in the sedimentary units M3c and M2c, cuts through M1c and extends down to the Si-metasomatised komatiitic flows (K). The stratigraphy is shown in Fig. 1b. Photos **(b)** and **(c)** are examples of black chert dikes cross cutting the volcaniclastic rocks of the upper Mendon formation.

SED
6, 1227–1264, 2014

Title Page
Abstract | Introduction
Conclusions | References
Tables | Figures
◀| |▶
◀ ▶
Back | Close
Full Screen / Esc
Printer-friendly Version
Interactive Discussion

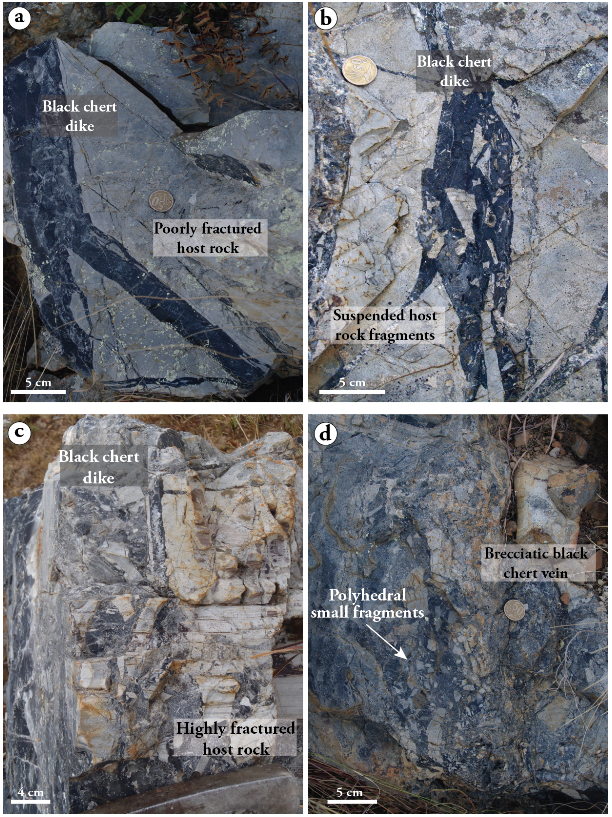

Fig. 4. Main types of dikes encountered in the Barite Valley syncline with degree of fracturation increasing from photo **(a)** to **(d)**. The fractures have straight and sharp **(a)** to irregular boundaries **(c)**. They contain variable amount of country rock fragments embedded in the black chert matrix, leading to clast-supported (**c** and **d**) or matrix-supported **(b)** textures in outcrop. Fragments are most commonly angular in shape.

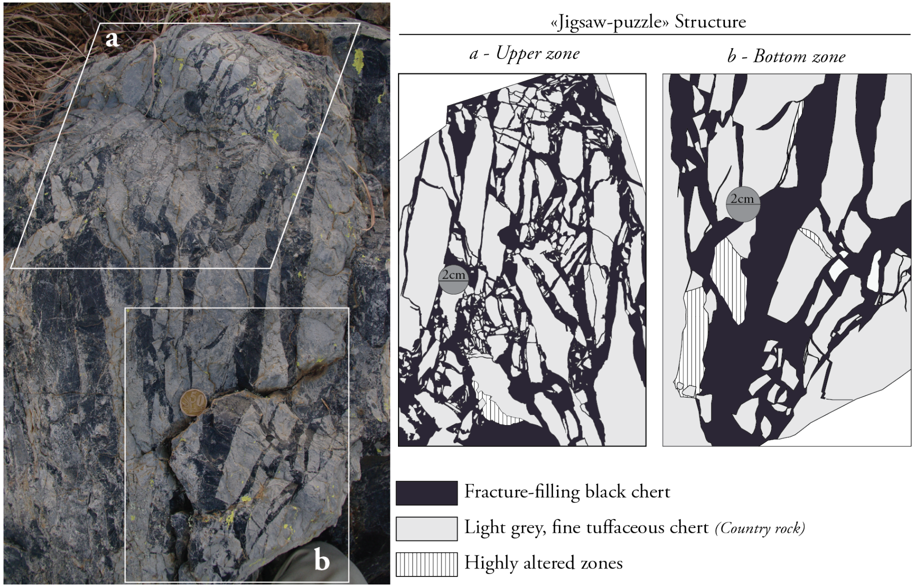

Fig. 5. Highly brecciated zone composed of long and angular host rock fragments with jigsaw fits separated by mm- to cm-thick black chert veins. The structures are more easily visible on sketches (**a** and **b**) corresponding to the upper and bottom parts of the structure respectively. **(a)** Rocks are fragmented in small blocks separated by thin black chert veins (< 1 mm–2 cm). Each block is minimally displaced. **(b)** This part of the outcrop is less fragmented and the black chert veins are thicker, reaching 4–5 cm. Note that the blocks present in the chert did not settle to the bottom part of the jigsaw structure. Instead, they look suspended in the siliceous matrix, at least in the two dimension view of the outcrop.

SED
6, 1227–1264, 2014

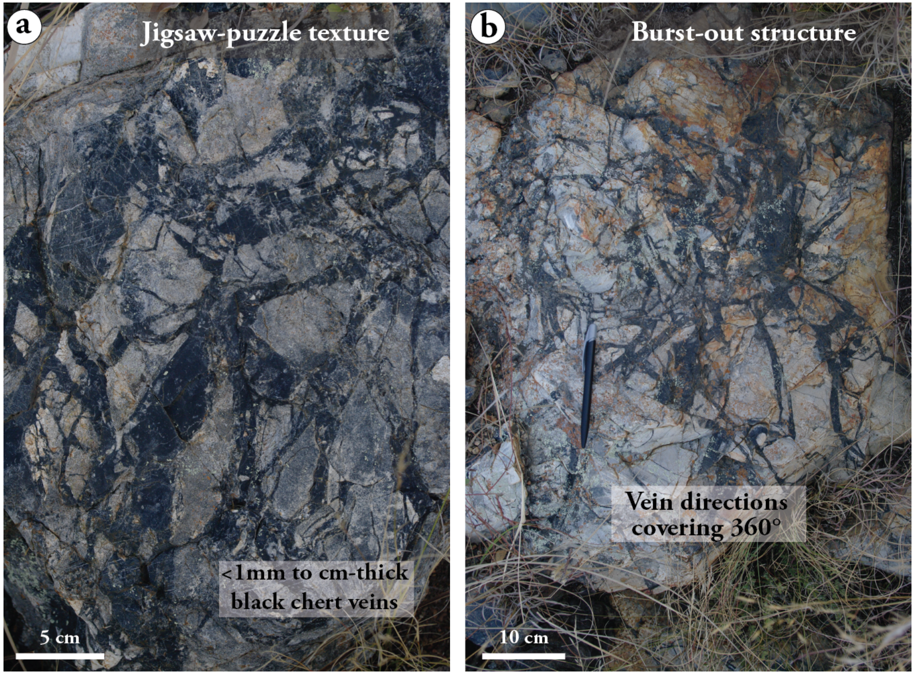

Fig. 6. Hydraulic-fracturation features in Barite Valley dikes. **(a)** Jigsaw-puzzle texture: angular and long-shaped country rock fragments little displaced and separated by cm-thick black chert veins. **(b)** Burst-out texture: radiating black chert veins at 360° around a central, highly fractured zone.

SED
6, 1227–1264, 2014

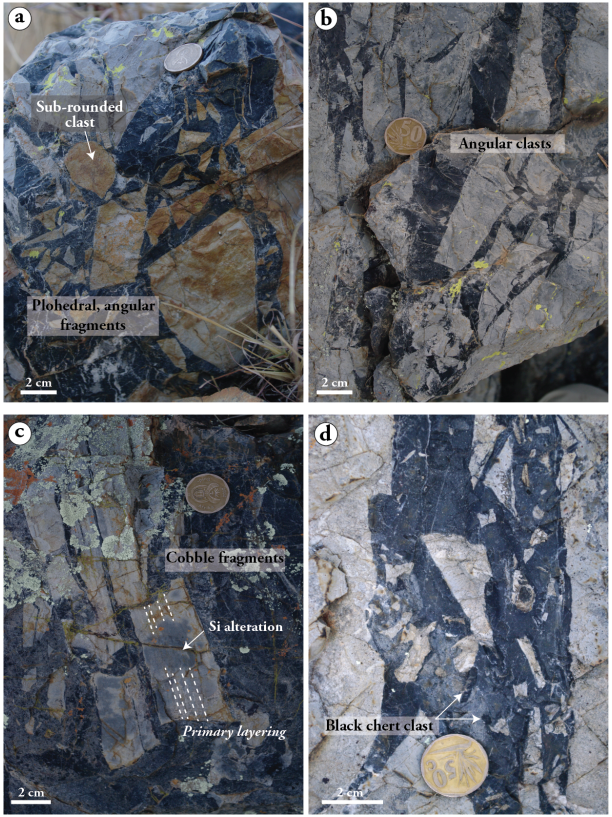

Fig. 7. Selection of dikes showing the most common shapes of country rock fragments. They range in size from < 1 cm to 40–50 cm (< 10 cm in average) and show a wide range of polyhedral shapes, from sub-rounded **(a)** to cobble-like **(c)**, the majority being highly irregular. More than 90 % of embedded fragments are from the surrounding host rock. The primary layering is generally well-preserved althought zones of silicification can be found **(c)**. The rest of fragments consists essentially of clasts eroded from older veins, such as the black chert clasts in **(d)**.

SED
6, 1227–1264, 2014

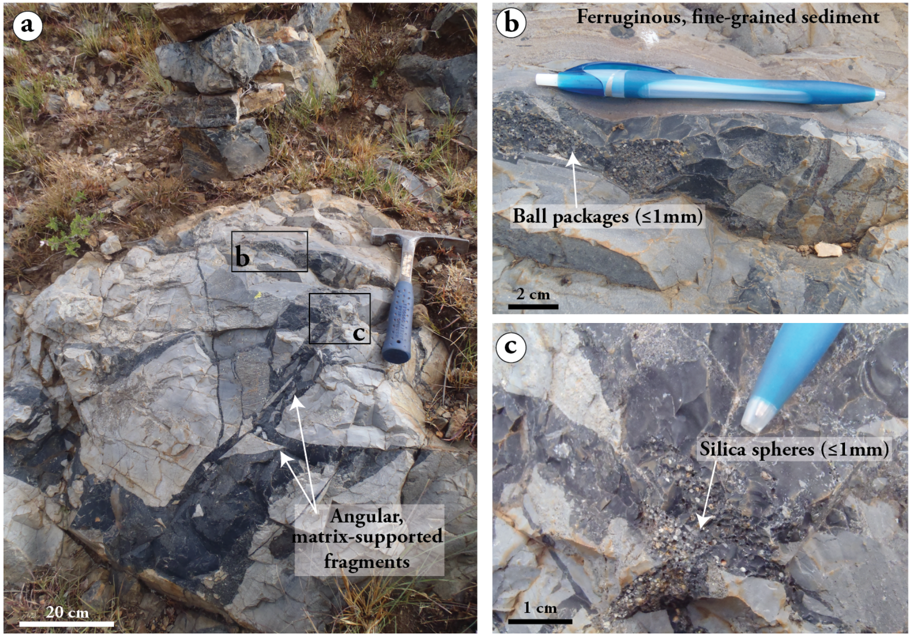

Fig. 8. (a) Homogeneous dike essentially filled of black chert with low amount of angular country rock fragments. Photos (**b** and **c**) are located in photo **(a)** and show agglomerates of small balls of translucent silica (< 1 mm). More than half of the balls were eroded during weathering and part of the remaining holes are now filled with modern zeolite. The packages are found at the bottom part of a black chert sill **(b)** or between suspended fragments in the main, vertical channel **(c)**.

SED
6, 1227–1264, 2014

The rheological behavior of fracture-filling cherts

M. Ledevin et al.

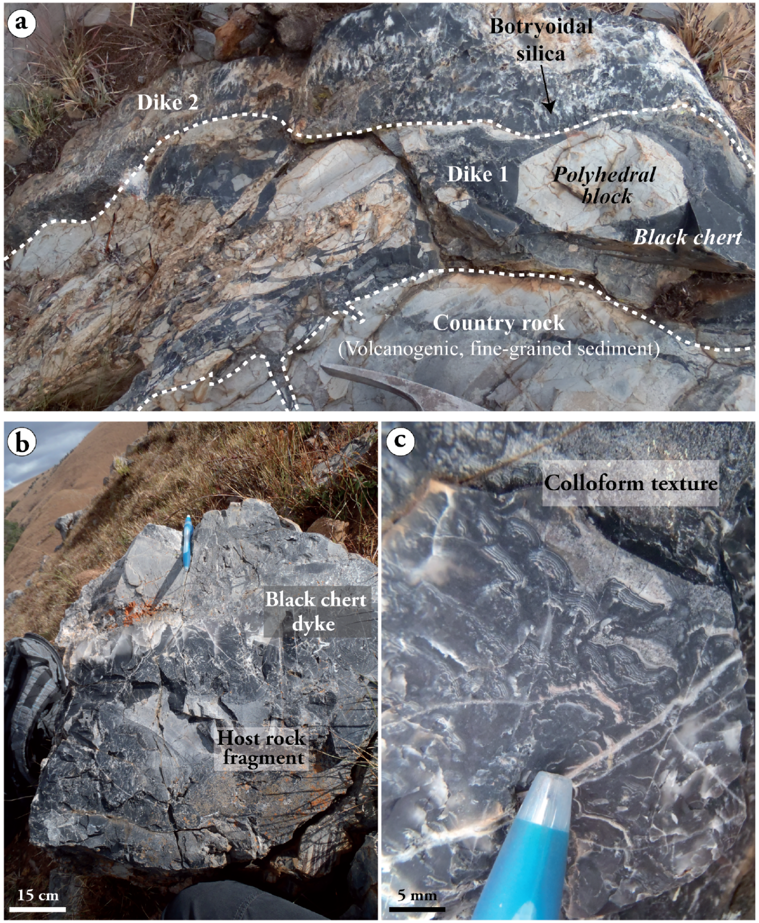

Fig. 9. Examples of dikes were host rock fragments are rare or absent. The silica precipitated to form either botryoidal columnar structures perpendicular to the fracture wall **(a)**, or colloform structures alternating thin black-and-white laminations (**b** and **c**).

SED
6, 1227–1264, 2014

The rheological behavior of fracture-filling cherts

M. Ledevin et al.

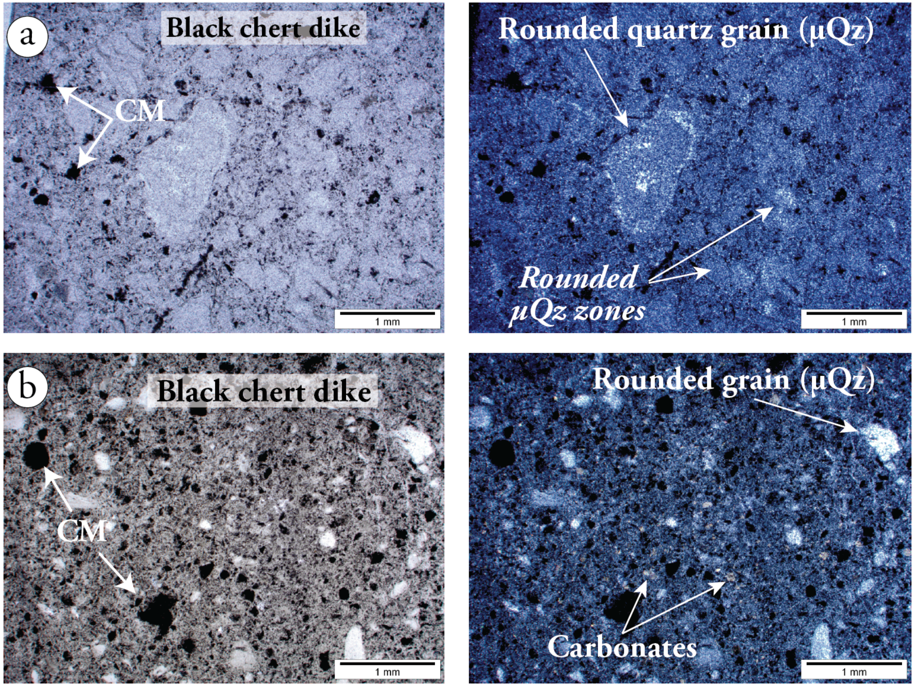

Fig. 10. Photomicrographs of fracture-filling black chert samples. CM = carbonaceous matter; µQz = microquartz. **(a)** Sample 1 composed of rounded particles of silica (> 70 % of the particulate fraction) and carbonaceous matter in a matrix of microquartz. The grains are 100–200 mm in average. Silica grains are composed of microquartz similar to the surrounding matrix leading to diffusive contact between both phases. Carbonaceous grains are aggregates of smaller particles. **(b)** Sample 2 composed of rounded particles of silica (50 % of the particulate fraction), carbonaceous matter (50 %) and carbonate (< 2 %) in a matrix of microquartz (up to 50–60 % of the chert).

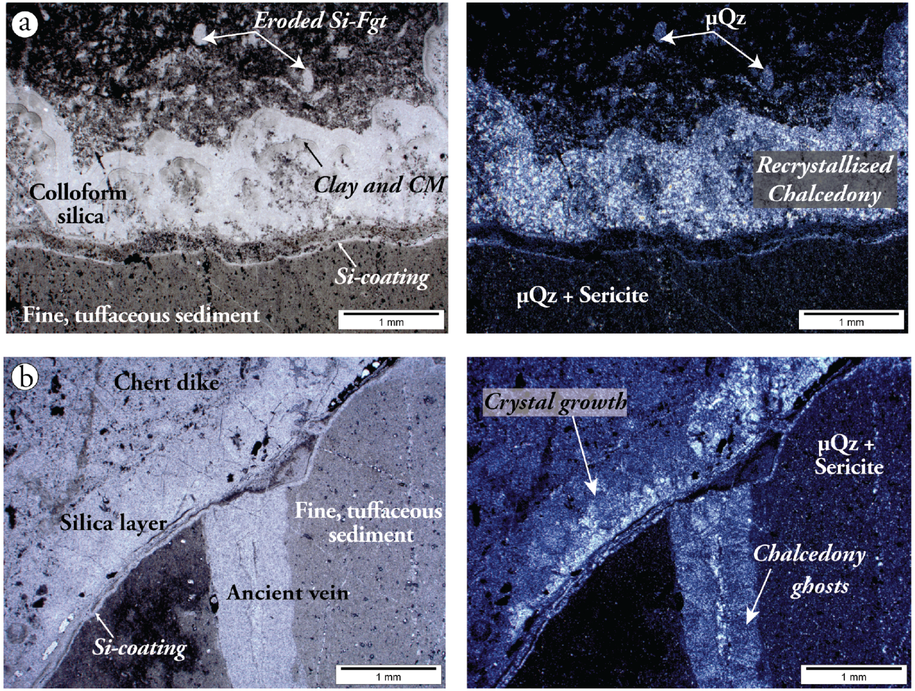

Fig. 11. Photomicrographs of fracture-filling black chert at the contact with country rocks. The contact is lined by < 1 mm -thick layers of nearly pure silica characterized either by colloform textures **(a)** or crystal growth structures perpendicular to fracture walls **(b)**.

SED
6, 1227–1264, 2014

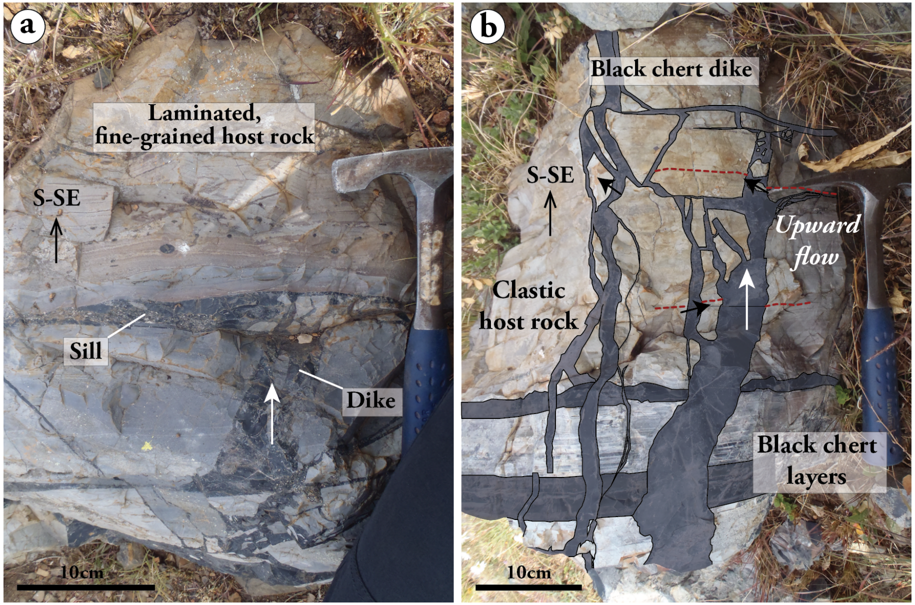

Fig. 12. (a) Dike-and-sill structure: a central, vertical channel spreads out laterally along weak sedimentary plane to produce sills concordant with country rock bedding. The structure ends in the younging direction by a final, < 5 cm-thick sill. **(b)** Vertical dike narrowing in the younging direction. Both photos are evidence for a migration of fluids from below.

SED
6, 1227–1264, 2014